

Light Source Notes

Assigned Number: LSBL-762

Date of Entry: 10/12/2005

Publishing Date: 10/10/2005

Author(s): S. C. Irick, W. R. McKinney, D. Peterman, V. V. Yashchuk

Title: Performance Test of Long Trace Profiler
Part 5.1: Noise due to Laser Pointing Instability

Other Number(s):

Performance Test of Long Trace Profiler

Part 5.1: Noise due to Laser Pointing Instability

Steve C. Irick^{a)}, Wayne R. McKinney^{a)}, Derrick Peterman^{b)}, Valeriy V. Yashchuk^{a)}

^{a)} *ALS ESG Optical Metrology Laboratory, Berkeley, 94720-8199*

^{b)} *Photon Inc., San Jose, 95119-1205*

October 10, 2005

Foreword to the Series

This Note continues a Series of works aimed (i) to investigate the performance of the existing LTP instrument as well as (ii) to determine its potential capabilities, and (iii) to lay out the measures and means for improvement of surface slope measurement with the LTP.

Preface to Part 5

In Part 1 [1], the random noise of the LTP measurement and its dependence on the laboratory environmental factors were investigated. It was shown that in a quiet laboratory environment, the random-noise limited accuracy of LTP measurements is on the level of $\sim 0.15 \mu\text{rad}$. That is the level of an acceptable sensitivity for a future generation LTP instrument. It was also demonstrated that the real problems of the existing LTP relate to systematic errors, which exceed the random noise by more than an order of magnitude.

In Part 2 [2], the problems of the LTP instrument related to the photo-detector were analyzed. It was found that a contribution in the detector systematic error of $\approx 0.6 \mu\text{rad}$ comes from the pixel-to-pixel photoresponse nonuniformity of the photo-diode array. A strong need was demonstrated for updating the LTP detector system with a system based on a CCD/PDA camera with higher pixel resolution. The update also should include a sophisticated calibration technique in order to gain maximum benefit from the new detector system.

In Part 3 [3,4], the efficiency of the data acquisition method and relevant software developed for suppressing the LTP systematic error related to the ‘ghost’ effect was demonstrated. The ‘ghost’ effect is an LTP systematic effect, arising due to partial superimposition of the reference and the sample light beams on the photo-detector. The effect is very pronounced when measuring the mirrors with relatively high sagittal curvature.

In Part 4 [5], questions related to the LTP fitting procedure are considered based on linear regression analysis. The consideration has allowed the development of an optimal fitting strategy and provided an analytical basis for estimation of the LTP performance as a function of the main LTP parameters.

In the present note, we describe the results of measuring pointing instability of different lasers. Included are an intensity stabilized He-Ne laser, a diode laser similar to one used in

the present version of the LTP, and a fiber coupled, temperature stabilized diode laser. The last laser in the list is being considered as a possible light source for the next generation of LTP instrument that is under development at the ALS OML.

The investigation of the LTP performance is not finished with this Note, but it will be continued in the next publications of the Series.

Contents

1. Introduction
2. Measurements of pointing instability of different lasers
 - 2.1. Fast measurements
 - 2.2. Measurement with averaging
 - 2.3. Temperature dependence of pointing stability of Melles Griot laser
3. Calculation of noise power density spectra due to laser pointing instability
4. Conclusions
5. Acknowledgements
6. References

1. Introduction

The pointing instability of a laser is determined as a temporal angular drift of the beam direction. In order to specify pointing instability of a laser, usual practice is to provide a value of change of the beam direction upon certain change of the ambient temperature in the units of rad/°C. Such specification of the pointing stability does not provide a laser user with adequate information on the temporal beam direction stability one can achieve. More adequate presentation of the pointing stability could be via an angular noise spectrum, similar to a noise power spectrum [6,7] usually used in electronics [8] or a power spectral density distribution applied to the surface roughness measurements [9].

In the case of a long trace profiler (LTP), such as one available at the ALS Optical Metrology Laboratory (OML) [1-5], rigorous information on the laser properties, is especially important. Indeed, the pointing instability of a light source used in the LTP directly

contributes into the instrumental noise of the slope trace measurements. Depending on the properties of the LTP detector (e.g., saturation intensity and related exposure time) and mode of the LTP measurement (e.g., possibility for multiple averaging of the interference features), different bandwidths of the laser angular noise spectrum contribute into the overall noise of the instrument.

In order to quantify pointing instability, an LTP with an additional reference beam was developed [10]. In the optical schematic of this instrument, the reference slope signal from a stationary reference mirror is recorded simultaneously with the slope trace measurement of a mirror under investigation. Then, the reference trace is subtracted from the sample trace, providing data basically free of error due to pointing instability. A similar approach has been used in a Dual-beam laser deflection sensor described in Ref. [11].

Unfortunately, the compensation of the laser pointing instability with a reference beam has some limitations. Indeed, the optical paths for the reference and the sample beams are significantly different. Moreover, the optical path for the reference beam is subject to change during the LTP measurement. As a result, the noise and systematic errors due to the imperfections of the LTP optics and convection of air along the optical paths are different for the reference and sample beams and can not be completely eliminated with the subtraction of the signals.

In the current version of the ALS LTP, a diode laser without active temperature stabilization but with a stabilized current power supply is used. The pointing stability for the laser is not specified in the available data sheet [12].

In the present report, we describe results of measuring the pointing instability of different lasers, including stabilized He-Ne laser [13], a diode laser, similar to one used in the present version of the LTP [12], and a fiber coupled, temperature stabilized diode laser (from Melles Griot Inc. [14]) being considered as a possible light source for the next generation of LTP instrument under development at the ALS OML.

2. Measurements of pointing instability of different lasers

The measurements were performed with a NanoScan sub-micron accuracy beam profiler (Photon Inc., [15]), when the instrument was demonstrated at the OML. The profiler (Fig. 1) is based on the slit-scanning method. At 3.5 mm aperture, the profiler comes with the 1.8 μm slits that are significantly smaller than the typical size of a pixel of a CCD or CMOS camera. The small slit width combined with high precision of the slit rotation provides an accuracy of 0.1 μm specified for the beam position measurements.

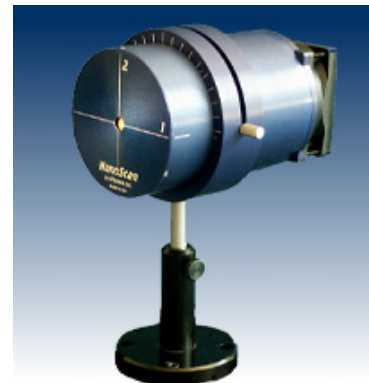


Figure 1: NanoScan beam profiler

The pointing stability was measured by observing a temporal dependence of a laser beam position detected with the profiler placed at a known distance from the laser. At the distance of 1 m, and 0.1 μm accuracy of a position measurement, the sensitivity to laser beam deflection is about 0.1 μrad . That is the desired pointing stability for the LTP laser.

2.1. Fast measurements

Figure 2 represents the temporal dependences of the beam position deviation from the averaged position for different lasers. All of the data in Fig. 2, except the profiler noise trace, were obtained at 1 m distance between a laser and the profiler. The sampling time for one point is 0.1 sec. The profiler noise was measured with the Melles Griot laser placed at the 10 cm distance, where the beam position deviation due to the laser pointing instability is suppressed by factor of ten. However, the standard deviation σ_x from the mean position was found to be changed only by approximately 30%. This suggests the profiler noise trace is mainly due to instrumental noise.

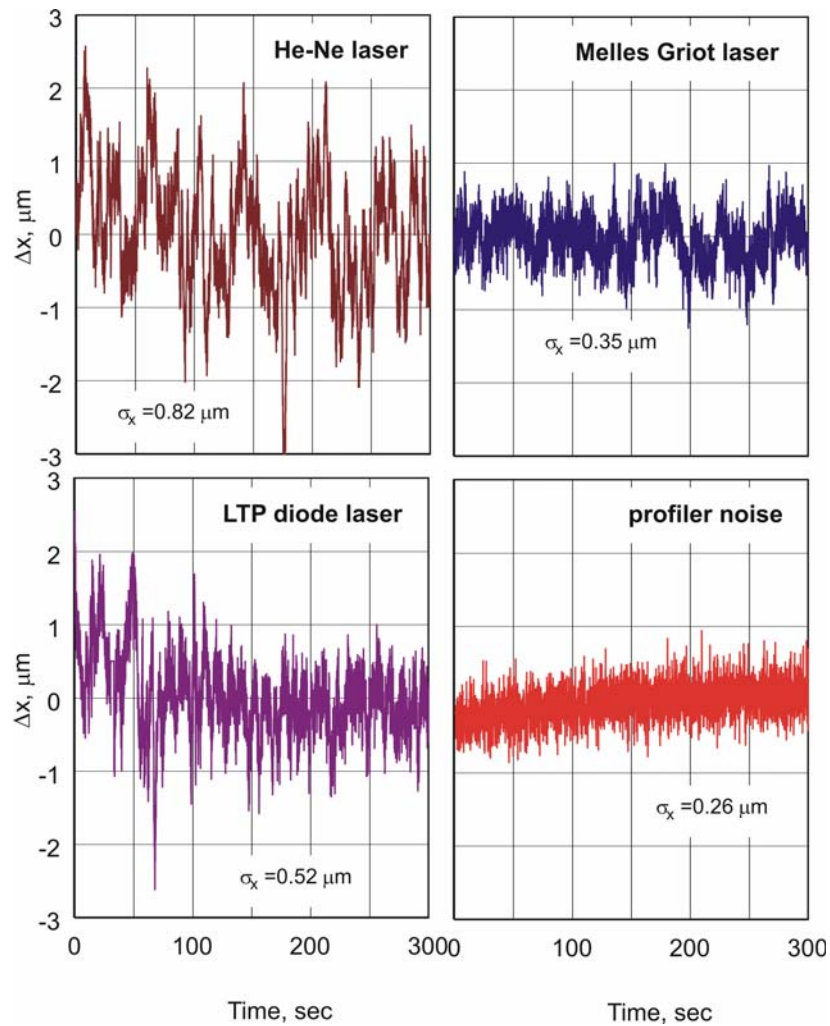


Figure 2: Temporal dependences of the beam position deviation from the averaged position for different lasers measured with sampling time of 0.1 sec.

The data shown in Fig. 2 were processed to get noise power density (NPD) spectra. The spectra presented in Fig. 3 have very similar behavior at frequencies from approximately 0.5 Hz and higher, where the noise is mainly due to instrumental noise. In this range, the instrumental noise has a white spectrum, which is suppressed significantly by averaging over a few measurements (see Sec. 2.2).

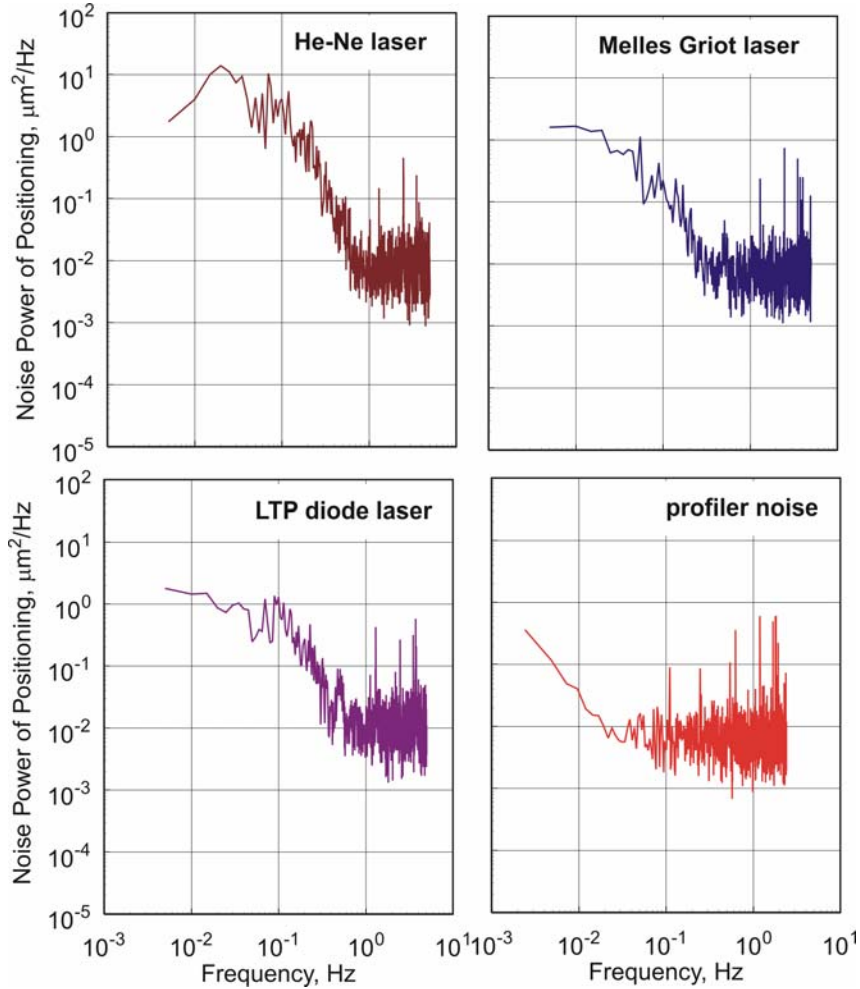


Figure 3: NPD spectra due to beam pointing instability for different lasers.

2.2. Measurement with averaging

A temporal sequence of the LTP trace scan consists of a number of sequential measurements with ~ 1 sec interval. The overall time range can be up to few thousand seconds depending on the size of the mirror. In order to be in congruence with the LTP arrangement, the measurements of the temporal dependences of the beam position for different lasers were carried out for a longer time range, more than 1200 s, and with averaging over 10 position measurements [16]. Figure 4 shows the results. Similar to Fig. 2, all of the data in Fig. 4 were obtained at 1 m distance between a laser and the profiler, except for the profiler noise trace, measured with the Melles Griot laser placed at the 10 cm distance.

As it was mentioned in the previous section, the random profiler noise is significantly, by factor of ~ 6 , suppressed by the averaging. The change in pointing stability (characterized with rms deviation) of the measured lasers is not so dramatic: $\sim 60\%$ decrease for the He-Ne laser, $\sim 45\%$ for the diode laser, and $\sim 35\text{-}40\%$ for the Melles Griot laser. Moreover, if one subtracts (using the quadratic subtraction usual for dispersions) the profiler rms noise for the measurements with the 0.1 s sampling time ($0.25\ \mu\text{m}$) from the corresponding data for beam pointing instability (Fig. 2), the change will be even smaller: $\sim 50\%$ decrease for the He-Ne laser, $\sim 25\%$ for the diode laser, and almost no improvement for the Melles Griot laser. However, one could naively expect the suppression to be a factor of ~ 10 for the all the lasers (as it is shown below, the effective integration time for the measurement with averaging was 10 sec).

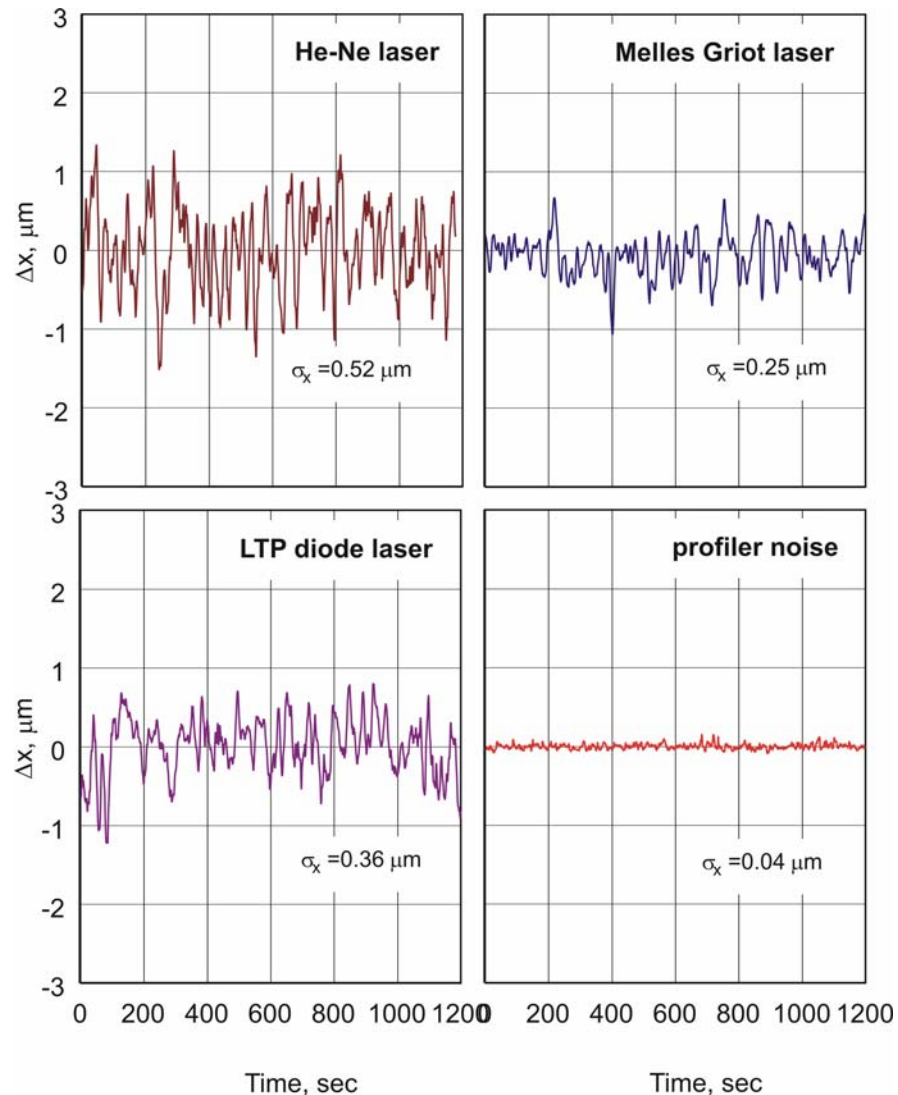


Figure 4: Temporal dependences of the beam position deviation from the averaged position for different lasers measured with averaging over 10 position measurements with time constant of 0.1 sec.

The NPD spectra (Fig. 5) transformed from the data in Fig. 4 help to resolve the problem. The spectra in Fig. 5 have very steep high frequency roll-offs. Due to the roll-off, the noise at frequencies, larger than ~ 0.1 Hz, does not contribute to the rms dispersion for the beam position. At very lower frequencies (less than ~ 0.03 Hz, the spectra correspond to white (random) noise of slightly different magnitudes. Averaging does not significantly affect this frequency range and, therefore, the change of position dispersion is very small. The air convection inside the hutch, surrounding the set-up, can significantly contribute in the noise in this frequency range.

There is a similarity in the high frequency spectra of Fig. 5. All of the spectra have characteristic, regularly displaced features. The similarity of the spectra can be thought as a manifestation of a characteristic instrumental function (analogous to the modulation transfer function used in optics) of the profiler, common for the measurements with averaging.

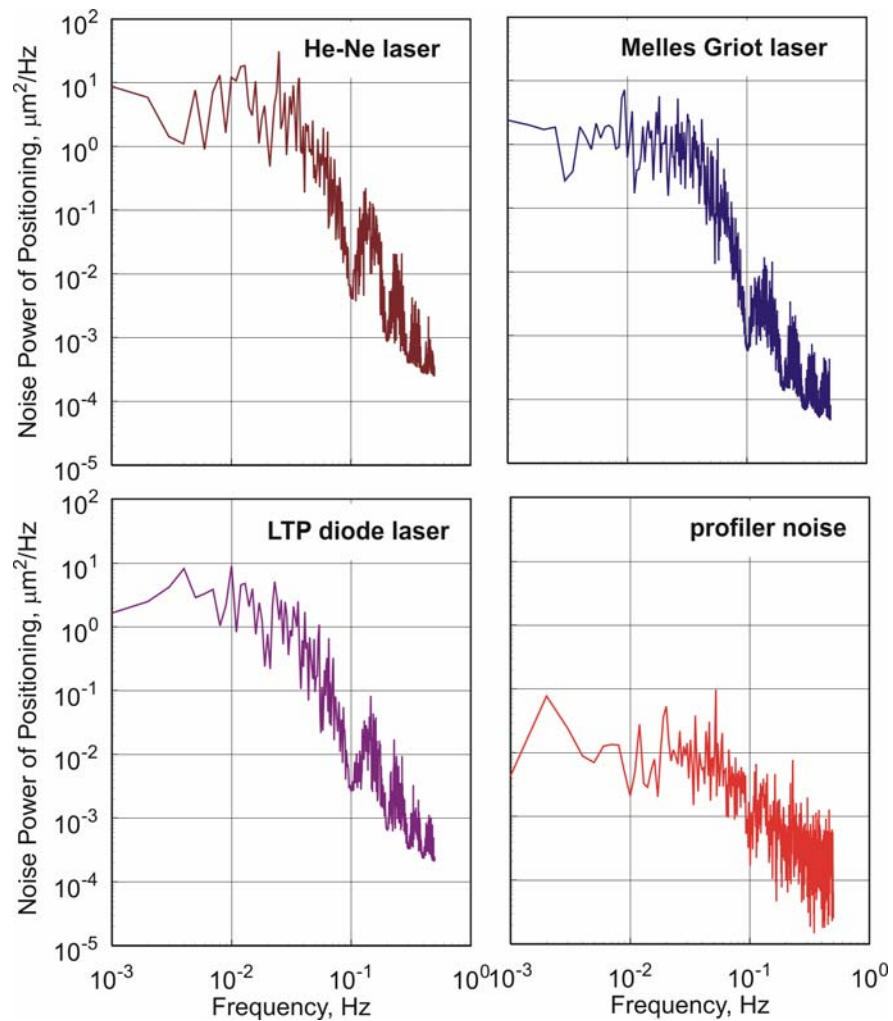


Figure 5: NPD spectra due to beam pointing instability for different lasers measured with averaging over 10 position measurements, each with time constant of 0.1 sec.

Figure 6 reproduces in a linear frequency scale the noise power spectrum (dark-red-colored trace), shown in Fig. 5 and measured with the Melles Griot laser. The spectrum has a characteristic beat, corresponding to a characteristic time $T_0 = 10$ sec. The bold light-red line fits the spectrum with averaging and corresponds to the function:

$$D(f) = \frac{\text{Sin}2(\pi T_0 f)}{(\pi T_0 f)^2} \cdot D_{fast}(f) + \text{const} . \quad (1)$$

The first product in the first term is a power spectral transformation of a rectangular gate function, natural for averaging:

$$W(t) = \begin{cases} 1, & |t| \leq T_0/2 \\ 0, & \text{elsewhere} \end{cases} . \quad (2)$$

The second product, $D_{fast}(f)$, is the NPD distribution measured without averaging (the blue traces in Fig. 3 and in Fig. 6). Note that the NPD spectrum without averaging has no beats. The constant, const , is introduced to account for random noise.

The irregularities of the fitted line (the bold light-red color in Fig. 6) are due to the spread of data of the fast measurement. But in any case, one can see a good agreement between the averaged measurement and the model given by (1) with $T_0 = 10$ sec and $\text{const} = 8 \cdot 10^{-5} \mu\text{m}^2/\text{Hz}$.

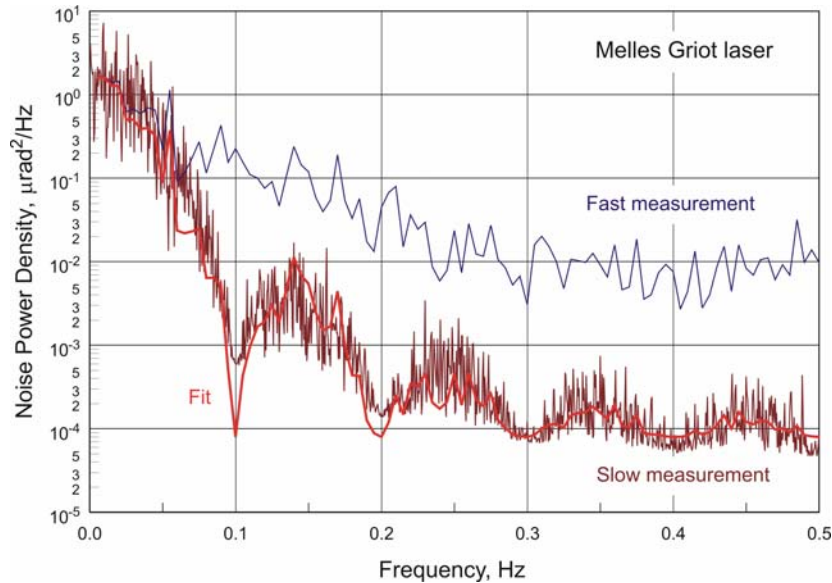


Figure 6: NPD spectra due to beam pointing instability for the Melles Griot laser: the red trace is measured with averaging over 10 position measurements, each with sampling time of 0.1 sec; the blue trace is the measurement without averaging; the red smooth line reproduces a fit of the averaged data to the function (1).

2.3. Temperature dependence of pointing stability of Melles Griot laser

The room temperature in the OML is controlled with a conditioner system, which provides temperature stability of $\sim 0.2^\circ\text{C}$ for a period of ~ 1 hours. However, right after switching the conditioner on or off, the room temperature drifts significantly. For the present experiment, such a temperature drift was used in order to get an experimental limit on the temperature coefficient, ξ_T , for the pointing stability of the Melles Griot laser. The correlation between the beam position change and temperature drift measured by switching the air conditioner gives $\xi_T = (20 \pm 3) \mu\text{rad}/^\circ\text{C}$. This value significantly exceeds the temperature coefficient, $\xi_T < 1 \mu\text{rad}/^\circ\text{C}$, specified for the pointing stability of the Melles Griot laser.

Unfortunately, a sensor, which we used to monitor temperature inside the hutch, surrounding the set up, has a large mass and, therefore, a large time constant. A more sophisticated experiment should be carried out in order to get more reliable data on the temperature coefficient.

3. Calculation of noise power density spectra due to laser pointing instability

A measured temporal sequence $P_r(t_r)$ of N points total is transformed into a noise power density spectrum $D_s(f_s)$ via discrete Fourier transformation:

$$D_s(f_s) = \Delta t \cdot |\text{Fourier}(P_r(t_r))|^2 = \frac{\Delta t}{N} \sum_{r=1}^N P_r(t_r) \cdot \exp\{2\pi i(r-1)(s-1)/N\}, \quad (3)$$

where the same definition of discrete Fourier transformation as in MathematicaTM is used. The result of application of the transformation (3) to the data for the profile noise in Fig. 2 is shown in Fig. 7a. Due to the limit of the length of the temporal sequence measured, there is a large spread of data at higher frequencies. The limited sequence can be thought as a product of an unlimited sequence and a rectangular temporal window. Fourier transformation of a rectangular window gives the high frequency variations of a resulted noise power spectrum [17].

One of the common ways to decrease the variations is to use a specially shaped window with smooth sides. This approach has a disadvantage of arbitrariness of the window shape. There are dozens of windows commonly used and none of them has any physical reason for priority (see also discussion in Ref. [18]). And in any case, windowing leads to a significant perturbation of the spectra, which is demonstrated with the data shown in Fig. 6.

The amplitude of the variations can be statistically decreased by splitting an initial temporal sequence into two shorter sequences and averaging over two noise power spectra for each of the sequences. The efficiency of the procedure is illustrated in Fig. 7b. The cost of the averaging is the loss of the lowest frequency point of the initial spectrum. The initial sequence can be divided to larger number of subsequences providing more efficient averaging and leading to the loss of lower frequency points of the NPD spectra.

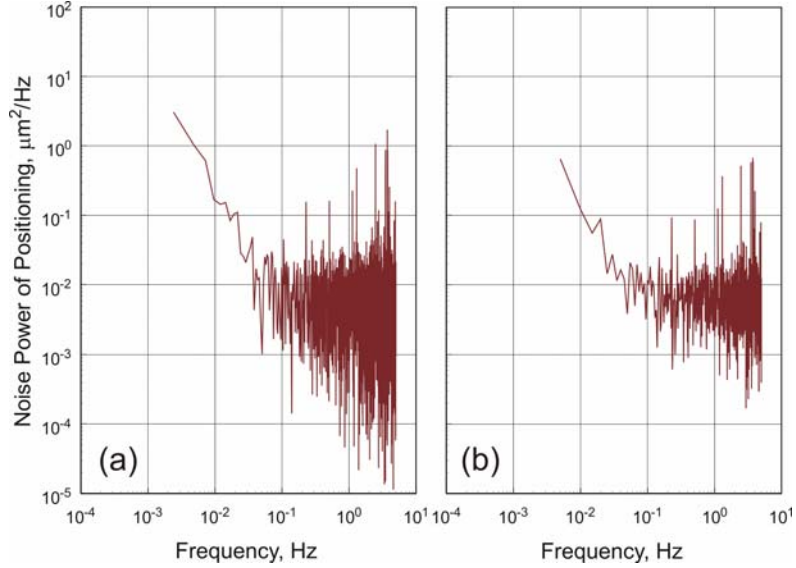


Figure 7: a – Noise power density spectrum obtained via discrete Fourier transformation (3) of the measured temporal sequence of the profiler position error (profiler noise); b – Noise power density spectrum averaged over two spectra, corresponding to two split sequences.

Even stronger suppression of the high frequency variations can be obtained with a simple procedure described in Ref. [18]. The technique is to partition the initial measured data into K subsequences, each of M consecutive measured points. The subsequences can overlap and, in this sense, they are not independent. Each subsequence is separately transformed into a NPD spectrum (3). Finally, the K spectra are averaged at each frequency to produce a spectrum with a reduction of the spread of high frequency data by factor of \sqrt{K} .

The described procedure with the parameters $M = K = N/2$, where $N \approx 4000$ is the length of the initial sequence that was applied to the profiler noise measurement shown in Fig. 2 and transformed into NPS presented in Fig. 7a. At the chosen parameters, the original data are partitioned into a set of subsequences sequentially shifted by one point as illustrated by Fig. 8.

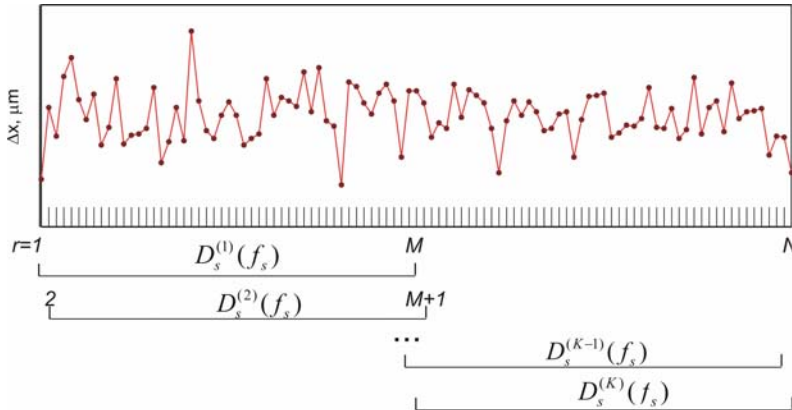


Figure 8: Illustration of the averaging procedure with partitioning into multiple dependent subsequences.

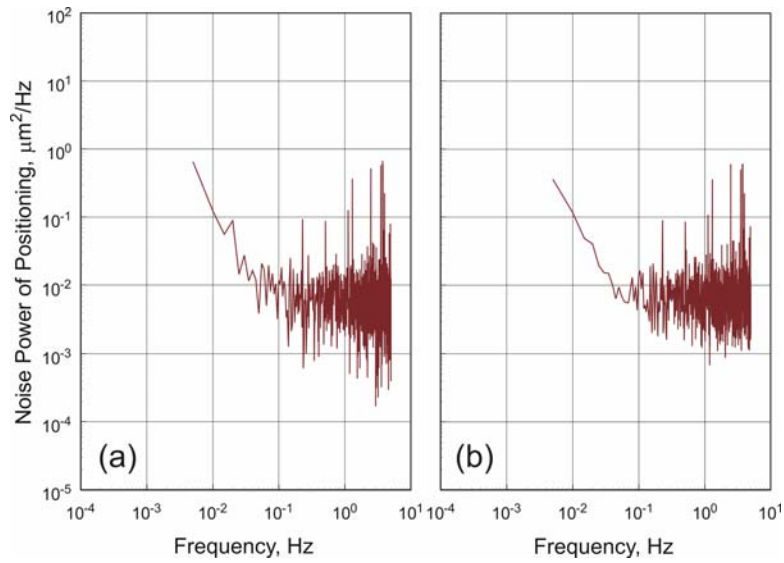


Figure 9: a – Noise power density spectrum averaged over two spectra, corresponding to two split sequences; b – Noise power density spectrum obtained with multiple averaging over shifted spectra.

The averaged spectrum is presented in Fig. 9b. The resulting variance at higher frequencies is even smaller than it is after averaging over two separated subsequences – Fig. 9a. the same averaging procedure was applied to the data shown in Figs. 3,5 and 6.

4. Conclusions

The performed experiments have shown a high performance of the NanoScan beam profiler (Photon Inc., [15]) and ability to measure a laser beam position with accuracy of $\sim 0.1 \mu\text{m}/\sqrt{\text{Hz}}$. This allows one to investigate the pointing instability of a laser with accuracy of $\sim 0.1 \mu\text{rad}/\sqrt{\text{Hz}}$ at the baseline of 1 m. Based on the result of the demonstration at the OML, the profiler system was purchased from the Photon Inc.

The profiler is useful for characterization of optical elements for metrology applications. For example, homogeneity of an optical element material (e.g., for beam splitters, etalon plates) can be verified by measuring the change of a laser beam position, while the element is accurately translated across the beam. The profiler can be used to investigate the effect of air convection along the optical path on the beam direction and to optimize the design of the optical path enclosure.

The procedure, similar to one applied to decrease the high frequency variance of the measured noise power density spectra, can be easily extended to the two-dimensional (2D) power spectral density (PSD) measurement the Micromap-570 interferometric microscope. In this case, a measured 2D height distribution is partitioned into a number of the

subdistributions. After processing each subdistribution with the PSD software developed at the OML [19-23], the obtained 2D PSD distribution would be averaged to suppress the high frequency noise.

The averaging procedure will save a significant amount of time, which we must spend on repeated measurements in order to provide the reliable 2D PSD data. The corresponding upgrade of the PSD software is planned.

5. Acknowledgements

The authors wish to thank to Alastair MacDowell for useful discussions.

The Advanced Light Source is supported by the Director, Office of Science, Office of Basic Energy Sciences, Material Science Division, of the U.S. Department of Energy under Contract No. DE-AC02-05CH11231 at Lawrence Berkeley National Laboratory.

Disclaimer

Certain commercial equipment, instruments, or materials are identified in this document. Such identification does not imply recommendation or endorsement by the US Department of Energy, LBNL or ALS nor does it imply that the products identified are necessarily the best available for the purpose.

6. References

1. V. V. Yashchuk, *Performance Test of the Long Trace Profiler. Part 1: Random Noise Limit of Slope Measurement with Mirror M4 for BL 9.0.2*, Light Source Note LSBL-710 (ALS, LBNL, Berkeley, August 06, 2004).
2. S. C. Irick, A. A. MacDowell, W. R. McKinney, and V. V. Yashchuk, *Performance Test of the Long Trace Profiler. Part 2: Systematic Errors of Slope Measurement Related to the Performance of the LTP Photo-detector*, Light Source Note LSBL-714 (ALS, LBNL, Berkeley, September 17, 2004).
3. S. C. Irick, A. A. MacDowell, and V. V. Yashchuk, *Performance Test of the Long Trace Profiler. Part 3: Removal of Systematic Error due to the 'Ghost' Effect*, Light Source Note LSBL-722 (ALS, LBNL, Berkeley, November 09, 2004).
4. V. V. Yashchuk, S. C. Irick, A. A. MacDowell, *Elimination of 'ghost'-effect-related systematic error in metrology of X-ray optics with a long trace profiler*, Proceedings of SPIE Symposium on Optical Metrology 2005, part of LASER2005, World of Photonics, (Munich, Germany, 12-17 June 2005), Proceedings of SPIE Vol. 5858, pp. 261-268 (SPIE, Bellingham, WA, 2005).
5. V. V. Yashchuk, *Performance Test of the Long Trace Profiler. Part 4: Estimation of Laser Beam Positioning Error*, Light Source Note LSBL-741 (ALS, LBNL, Berkeley, March 28, 2005).
6. M. C. Geckini and D. Yavus, *Discrete Fourier Transformation and Its Applications to Power Spectra Estimation* (Elsevier scie. Publ. Co., Amsterdam, 1983).

7. R. N. Bracewell, *The Fourier Transform and Its Applications* (Tata McGraw-Hill Publ. Co. Ltd., New York, 2003).
8. P. Horowitz and W. Hill, *The Art of Electronics* (Cambridge Univ. Press, New York, 1994).
9. J. C. Stover, *Optical Scattering: Measurements and Analysis* (SPIE, Washington, 1995).
10. S. C. Irick, *Improved measurement accuracy in a long trace profiler: compensation for laser pointing instability*, [Conference Paper] Nucl. Instrum. & Meth. A 347(1-3), 226-30 (1994).
11. Pawliszyn J, Weber MF, Dignam MJ. *Dual-beam laser deflection sensor*, Rev. Sci. Instrum. 56(9), 1740-3 (1985).
12. Optima Model CDL3605-672, 670 nm, 2.5 mW, collimated laser diode (based on Toshiba TOLD 9211S laser diode).
13. Spectra-Physics Stabilized He-Ne laser – Model 11A (http://www.newport.com/file_store/Data_Sheet/117A_Datasheet.pdf).
14. Melles Griot 57 ICS-Series Fiber-Coupled 670 nm, 3 mW, Diode Lasers Module (<http://lasers.mellesgriot.com/Specsheet.asp?CatID=11521>).
15. Photon Inc., *NanoScan: High-Power Sub-Micron Accuracy Beam Profiler* (<http://photon-inc.com>).
16. In the course of demonstration, we tried to arrange the measurement with averaging over 10 position measurements, each with time constant of 0.1 sec. Thus, the integration time was desired to be 1 sec. In reality, the integration time appeared to be 10 sec that is shown in Sec. 2.2.
17. N. C. Geckinli and D. Yavuz, *Discrete Fourier Transformation and Its Applications to Power Spectra estimation* (Elsevier, New York, 1983).
18. W. H. Press, S. A. Teukolsky, W. T. Vetterling, B. P. Flannery, *Numerical Recipes in C++: The Art of Scientific Computing* (Second Ed., Cambridge Univ. Press, Cambridge, 2003).
19. V. V. Yashchuk, A. D. Franck, S. C. Irick, M. R. Howells, A. A. MacDowell, W. R. McKinney, "Two dimensional power spectral density measurements of X-ray optics with the Micromap interferometric microscope," in *Nano- and Micro-Metrology*, H. Ottevaere, P. DeWolf, D. S. Wiersma, eds., Proc. SPIE **5858**, 85-96 (2005).
20. V. V. Yashchuk, S. C. Irick, E. M. Gullikson, M. R. Howells, A. A. MacDowell, W. R. McKinney, F. Salmassi, T. Warwick, "Crosscheck of different techniques for two dimensional power spectral density measurements of X-ray optics," in *Advances in Metrology for X-Ray and EUV Optics*, L. Assoufid, P. Z. Takacs, J. S. Taylor, eds., Proc. SPIE **5921**, 105-116 (2005).
21. Valeriy V. Yashchuk, Eric M. Gullikson, Malcolm R. Howells, Steve C. Irick, Alastair A. MacDowell, Wayne R. McKinney, Farhad Salmassi, Tony Warwick, James P. Metz and Thomas W. Tonnessen, *Surface Roughness of Stainless Steel Bender Mirrors for Focusing Soft X-rays* (submitted to Applied Optics, October, 2005).